Tailoring immobilization of immunoglobulin by excimer laser for biosensor applications

Felix Sima,[1] Emanuel Axente,[1] Carmen Ristoscu,[1] Ion N. Mihailescu,[1] Taras V. Kononenko,[2] Ilya A. Nagovitsin,[2,3] Galina Chudinova,[2] Vitaly I. Konov,[2] Marcela Socol,[4] Ionut Enculescu,[4] Livia E. Sima,[5] Stefana M. Petrescu[5]

[1]National Institute for Lasers, Plasma and Radiation Physics, Magurele, Ilfov, Romania
[2]Natural Sciences Center of A. M. Prokhorov General Physics Institute RAS, Moscow, Russia
[3]N. N. Semionov Institute of Chemical Physics RAS, Moscow, Russia
[4]National Institute of Materials Physics, Magurele, Ilfov, Romania
[5]Institute of Biochemistry, Romanian Academy, Splaiul Independentei 296, Bucharest, Romania

Received 6 August 2010; accepted 5 October 2010
Published online 8 December 2010 in Wiley Online Library (wileyonlinelibrary.com). DOI: 10.1002/jbm.a.32991

Abstract: The sheltered transfer and immobilization of rabbit anti-human antiserum immunoglobulin G (IgG) by matrix-assisted pulsed laser evaporation (MAPLE) are reported. The iced targets submitted to laser irradiation consisted of 0.2–2 mg/mL IgG blended or not with lipid (L-α-phosphatidylcholine dipalmitoyl) dissolved in distilled water-based saline buffer. Thin IgG coatings were obtained at room temperature onto glass, fused silica, or silicon substrates. Ten thousand subsequent laser pulses of 0.33, 0.5, or 0.67 J/cm^2 fluence were applied for the synthesis of each sample. Morphology and composition of the thin films were studied by optical, scanning, and atomic force microscopy and Fourier transformed infrared spectrometry. Optical labeling methods such as spectrofluorimetry and fluorescence microscopy were selected to verify the biosensor transduction principle because of their high sensitivity for detecting low amounts of antigen (IgG). Protein immobilization to the substrate surface was demonstrated for all obtained structures after immersion in the donkey anti-rabbit secondary antibody solution. The IgG transfer and immobilization onto substrates were improved by addition of lipid to MAPLE solutions. J Biomed Mater Res Part A: 96A: 384–394, 2011.

Key Words: biosensors, immunodetection, immunoglobulin, laser immobilization

INTRODUCTION

Immunoreceptors stand for the main category of biological detection elements for biosensor applications. The antibodies are selective and chemical affinity molecules produced by B lymphocytes in response to the introduction of a foreign molecule (antigen) in the body. An antigen is a substance that elicits antibody generation and reacts specifically with that antibody. Because the antibody–antigen reaction is highly specific, each molecule can serve as a unique chemical detector for the other.

The immobilization of proteins and, in particular, of immunoglobulins, in thin films or nanostructures, is a real challenge and of great interest for the development of miniaturized biosensors based on the immediate reaction between the antibody and the antigen.

Two of the most well-known techniques for protein immobilization methodically similar to our approach are electrostatic layer-by-layer (LbL)[1,2] and Langmuir–Blodgett (LB)[3] methods, which act complementary for different types of materials. Although in the case of LbL one can use alternating layers of water-soluble materials with negative and positive charges, LB is used for the preparation of thin films on solid substrates and proceeds by the transfer of the films insoluble in water from air/water interface.

At present, many other immobilization techniques were applied in view of increasing the adhesion of the layers to the substrate. The surface functionalization,[4] complex biological interactions between biotin and avidin[5] and proteins A or G,[6,7] chemical interactions as glutaraldehidic or 1,-4 phenylene diisothiocyanate bonding,[8–11] and physical adsorption[12] were tested to find the best possible compromise and optimize the protein immobilization to different supports. It was demonstrated that the protein immobilization depends on surface properties such as composition, reactivity, wettability, and roughness.[13,14]

Matrix-assisted pulsed laser evaporation (MAPLE) method was developed to surpass the difficulties related to photonic and thermal damages of fragile organic materials under intense laser irradiation.[15,16] In respect with the well-known conventional technologies used for protein

Correspondence to: I. N. Mihailescu; e-mail: ion.mihailescu@inflpr.ro
Contract grant sponsor: Romanian Academy; contract grant numbers: GAR6/2008, 5/2009
Contract grant sponsor: Russian Foundation for Basic Research; contract grant number: 93106
Contract grant sponsor: UEFISCSU; contract grant number: IDEI 511/2009

TABLE I. Experimental Conditions for the Examined IgG Samples

Sample	Fluence (J/cm^2)	Buffer Solution	Optimized Parameters in the Reaction Chamber (Temperature, Pressure, Target-Substrate Separation Distance)
I33	0.33	Distilled water/TRIS/NaCl	RT, 0.1 Torr, 4 cm
I50	0.5	Distilled water/TRIS/NaCl	RT, 0.1 Torr, 4 cm
I67	0.67	Distilled water/TRIS/NaCl	RT, 0.1 Torr, 4 cm
IL33	0.33	Distilled water/TRIS/NaCl + lipid[a]	RT, 0.1 Torr, 4 cm
IL50	0.5	Distilled water/TRIS/NaCl + lipid[a]	RT, 0.1 Torr, 4 cm
IL67	0.67	Distilled water/TRIS/NaCl + lipid[a]	RT, 0.1 Torr, 4 cm

[a] L-α-phosphatidylcholine dipalmitoyl.

immobilization, MAPLE presents some distinctive advantages.[17] It thus allows for controlling the thickness of the layer from a few to hundreds of nm, permits the relatively uniform spreading of material over rather large areas, and can be extended to the synthesis of multistructures. Multicomponent targets (containing proteins and other functional materials) can be easily prepared and used for synthesis of layers with superior stability and adhesion to substrate. MAPLE proved successful for the deposition of thin layers of organics and biomaterials such as biopolymers,[18,19] enzymes,[20,21] and other proteins.[22]

We extended and report herewith the application of MAPLE to the transfer and immobilization of immunoglobulin G (IgG) molecules onto glass, fused silica, or silicon. We investigated the influence of the incident laser fluence and the effect of the lipid addition in the initial solution upon the protein thin films adhesion to substrates.

MATERIALS AND METHODS

Thin films of immunoglobulin have been deposited by MAPLE onto glass, fused silica, or silicon substrates because they were considered attractive support materials for IgG immobilization by adsorption.[23] Before deposition, the substrates were cleaned in an ultrasonic bath subsequently in acetone, ethyl alcohol, and deionized water. The solutions consisting of 0.2–2 mg/mL IgG in distilled water and saline buffer (TRIS 50 m*M*, pH 7.4, NaCl 150 m*M*) were homogenized and frozen at 77 K in liquid nitrogen. After freezing, the solid target was mounted inside a reaction chamber and rotated with 10 rpm to avoid overheating and drilling due to multipulse laser irradiation. The targets were maintained frozen during the laser irradiation by a cooler device filled continuously with liquid nitrogen. The experiments were performed at room temperature in a dynamic pressure of 0.1 Torr. The target–substrate separation distance was found optimal at 4 cm. A pulsed KrF* laser source ($\lambda = 248$ nm, $\tau_{FWHM} \approx 25$ ns) operating at 15 Hz was used for the target evaporation. Ten thousand subsequent pulses at 0.33, 0.5, or 0.67 J/cm^2 incident laser fluence were applied for the synthesis of each structure. We note that this level of fluence is about one order of magnitude lower than in conventional pulsed laser ablation or deposition of inorganic materials, a safety assessment adopted for the protection of IgG molecules against laser beam irradiation. During multipulse laser deposition, the substrates were translated along two orthogonal axes to ensure the synthesis of a highly uniform film.

To obtain protein–lipid mixture, we used 1 m*M* ethanol solution of lipid—L-α-phosphatidylcholine dipalmitoyl (Sigma-Aldrich); well-defined amounts were added in water-buffered solution–IgG mixtures. The ethanol solutions of lipid were prepared by lipid dissolution in several microliters of chloroform (spectroscopy grade, Uvasol) and subsequently adding 1–5 mL ethanol under intensive mixing.

Table I collects the representative experimental conditions in this study.

The surface morphology of the synthesized films was examined by optical and atomic force microscopy (AFM) in tapping mode with a Nanonics MV 4000TM Microscope and by scanning electron microscopy (SEM) using a Carl Zeiss EVO microscope.

Fourier transform infrared (FTIR) spectrometry analysis was carried out in transmission mode with a FTIR Shimadzu 8400S instrument within the range of interest 4000–1200 cm^{-1}.

Spectrofluorimetry and fluorescence microscopy investigations were performed for detecting the low amounts of antigen (IgG). The rabbit serum was evidenced by an Alexa Fluor 488-conjugated donkey anti-rabbit secondary antibody (Molecular Probes). Before incubation with a 1:50 dilution of antibody, the samples were immersed for 30 min in a 0.5% bovine serum albumin (BSA)–PBS solution at room temperature to block free binding sites. This prestaining step assured the specific binding of the fluorescent antibody to the IgG fraction of rabbit antiserum. After thoroughly washing the samples in PBS, 10 × 10 fields were scanned using a Mithras spectrofluorimeter (Berthold), and the fluorescence intensity was quantified at 530 nm. Samples were also analyzed in a Nikon TS100 epifluorescence microscope, and images were captured with the NIS Elements software.

Next, we used a BCA (bicinchoninic acid) protein assay (Thermo Scientific) to quantify the amount of IgG on substrates. The proteins were removed from their sites by incubation in a buffer solution of 10 m*M* Tris and 1 m*M* EDTA for 6 h at 4°C.[24] The determined concentration of IgG in supernatant was then normalized to the surface of the structure to obtain the amount of protein deposited per unit surface area (cm^2).

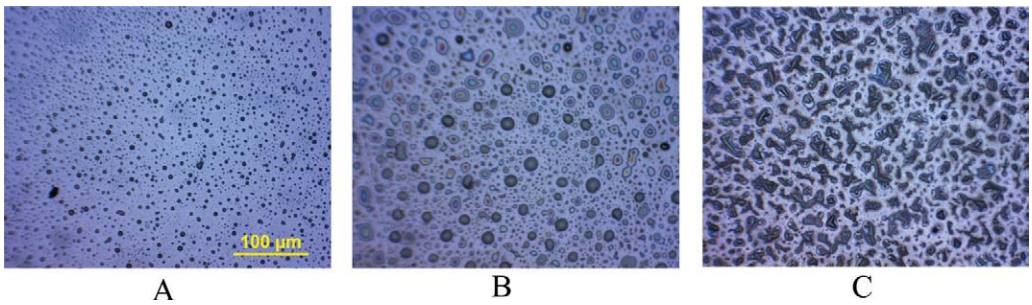

FIGURE 1. Optical images (×100) of IgG structures obtained by MAPLE deposition on fused silica substrates from IgG dissolved in water and saline buffer without lipid at fluences of (A) 0.33 J/cm^2 (I33), (B) 0.5 J/cm^2 (I50), and (C) 0.67 J/cm^2 (I67), respectively. [Color figure can be viewed in the online issue, which is available at wileyonlinelibrary.com.]

RESULTS

The immobilized structures were characterized by physico-chemical studies and antibody assays.

Optical microscopy

The optical examination of the transferred structures showed important differences of the IgG organization on all substrates versus incident laser fluence (Figs. 1 and 2). We thus noticed a spot-like configuration in the case of the protein transferred at the lowest fluence [I33—Fig. 1(A)], most probably because of the small quantity of immobilized material. When increasing the laser fluence (I50), larger round structures with a relative good distribution over the substrate surface were formed [Fig. 1(B)]. At a higher fluence (I67), more material was deposited but presenting irregular structure [Fig. 1(C)] perhaps because of the significant quantity of the transferred salts from the IgG buffered solution.

A similar evolution of the deposited IgG-lipid structures function of incident transfer fluence was recorded with relevant morphological peculiarities when increasing the laser energy (Fig. 2). The distribution obtained for IL33 was spot like [Fig. 2(A)], comparable to I33 in Figure 1(A). The optical images corresponding to the structures IL50 exhibited a well-protected, encapsulate-like material [Fig. 2(B)], when compared with I50 in Figure 1(B), where splashed and broken particulates could be seen besides intact ones. The optical evidence for the IL67 [Fig. 2(C)] was equivalent to that of I67. Nevertheless, additional irregular structures can be noticed over the entire area.

Atomic force microscopy

The tapping mode used in AFM investigations was a real advantage, which allowed us to touch and withdraw from the sample surface continually avoiding the sample damage but making possible the high resolution of contact mode. The results of AFM investigations were to some extent congruent with the information from optical microscopy examinations. Some typical recordings for an investigation area of 40 × 40 μm^2 are given in Figures 3 and 4 for structures deposited without or with lipid addition. The corresponding profile roughness parameters, that is, root mean squared (RMS), roughness arithmetic average (Ra), and the average height (Rz) values inferred from Figures 3 and 4 for all samples, are collected in Table II.

We observed that in the case of IgG structures obtained from solutions without lipid (Fig. 3), RMS, Ra, and Rz values present a maximum for I50. On the other hand, in case of lipid addition (Fig. 4), these values continuously increased from IL33 to IL67.

Scanning electron microscopy

We presented in Figures 5–7 typical SEM micrographs recorded for IgG structures obtained from solution without lipid (I) and containing lipid (II). One first observation is the relative good correlation between optical microscopy, AFM, and SEM evidences obtained for all samples. Thus, the spot-like structures corresponding to 0.33 J/cm^2 fluence are equally visible for I33 and IL33 (Fig. 5), whereas a rather irregular, quasi-continuous film formed of protein and large

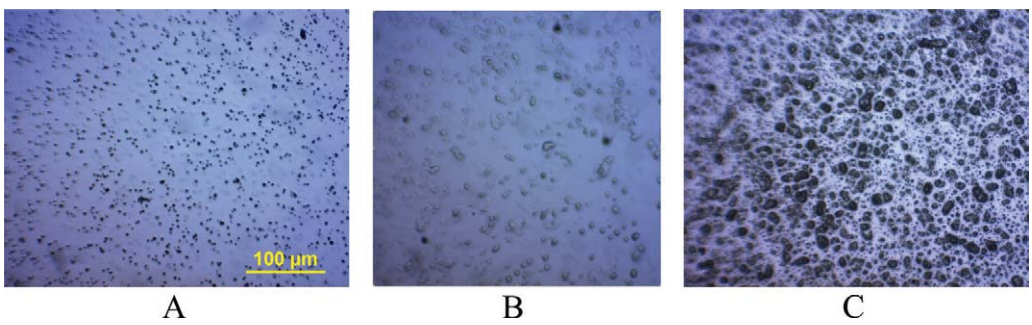

FIGURE 2. Optical images (×100) of IgG structures obtained by MAPLE deposition on fused silica from IgG dissolved in water and saline buffer containing lipid at fluences of (A) 0.33 J/cm^2 (IL33), (B) 0.5 J/cm^2 (IL50), and (C) 0.67 J/cm^2 (IL67), respectively. [Color figure can be viewed in the online issue, which is available at wileyonlinelibrary.com.]

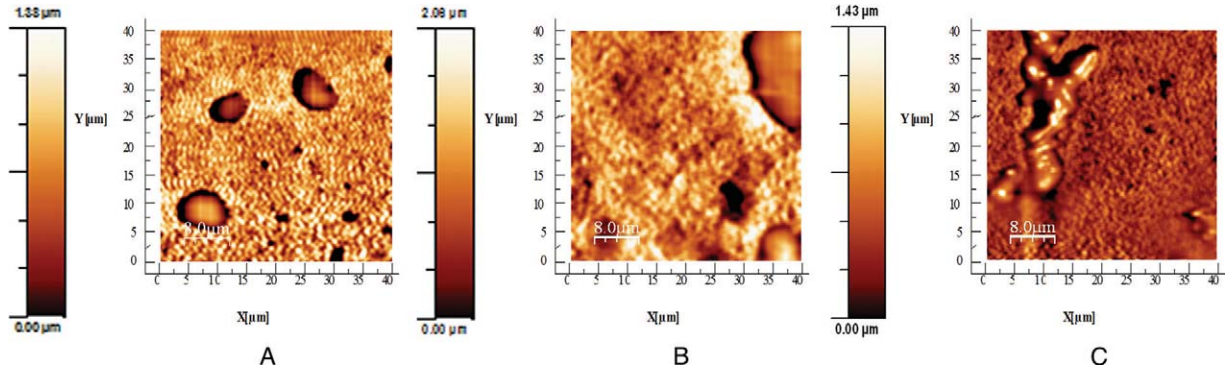

FIGURE 3. AFM images of IgG structures obtained by MAPLE deposition on fused silica substrates from IgG dissolved in water and saline buffer without lipid at fluences of (A) 0.33 J/cm^2 (I33), (B) 0.5 J/cm^2 (I50), and (C) 0.67 J/cm^2 (I67), respectively. [Color figure can be viewed in the online issue, which is available at wileyonlinelibrary.com.]

quantities of salts were characteristic to the other structures (Figs. 6 and 7). Higher was the fluence, more salts were noticed with important quantity of transferred material when using lipid. The significant difference between IL50 and IL67 is the relatively superior protection and well-defined transfer of the IgG biomolecules in the first case, whereas a more complex microrelief due to intense expulsion of buffer salts could be noticed in the second one. This latter feature supports the high roughness values obtained by AFM. IgG fibrils are visible in Figure 6(IIa) proving the safe transfer of proteins from solution to substrate. Conversely, amounts of crystalline salts are observed in Figure 7, visibly larger in the case of samples obtained from solutions with lipid [Fig. 7(II)].

Fourier transform infrared spectroscopy

The congruent transfer by MAPLE of IgG molecules from the frozen target to substrate was sustained by FTIR. To discriminate between the different compound spectra, we investigated separately silicon, saline buffer dropcasts, and lipid, respectively. The recorded absorption spectra are given in Figure 8. Common absorption bands of saline buffer and lipid were noticed within the ranges 1500–1400 cm^{-1}, 2000–1800 cm^{-1}, and 3000–2200 cm^{-1}.

One can observe from Figure 9(A) that the spectra of I50 and I63 well reproduced the dropcast, whereas in I33 spectrum the important lines of protein absorption at 2962 and 3280 cm^{-1} were missing. Accordingly, the transfer could be considered congruent at incident fluences of 0.5 and 0.67 J/cm^2, but deficient at 0.33 J/cm^2. The lowest laser fluence was apparently too weak to promote the transfer of the protein. The I50 spectrum exhibited higher intensity absorption bands, the most likely indicative for a larger amount of integer IgG. These results confirmed the microscopically evidence that the optimal transfer was obtained under the action of 0.5 J/cm^2 laser fluence.

Comparable development was noticed when the starting mixture contained lipid. The similitude between the dropcast and thin films was observed from the spectra recorded in Figure 9(B). In addition, the most intense spectrum was recorded in case of the film deposited with 0.5 J/cm^2, which confirmed that this fluence ensured the optimal transfer of IgG molecules.

Antibody assays

To circumvent the nonspecific reactions, various dilutions of Alexa Fluor 488 donkey anti-rabbit secondary antibody (2 mg/mL) were tested in blocking buffer to determine the

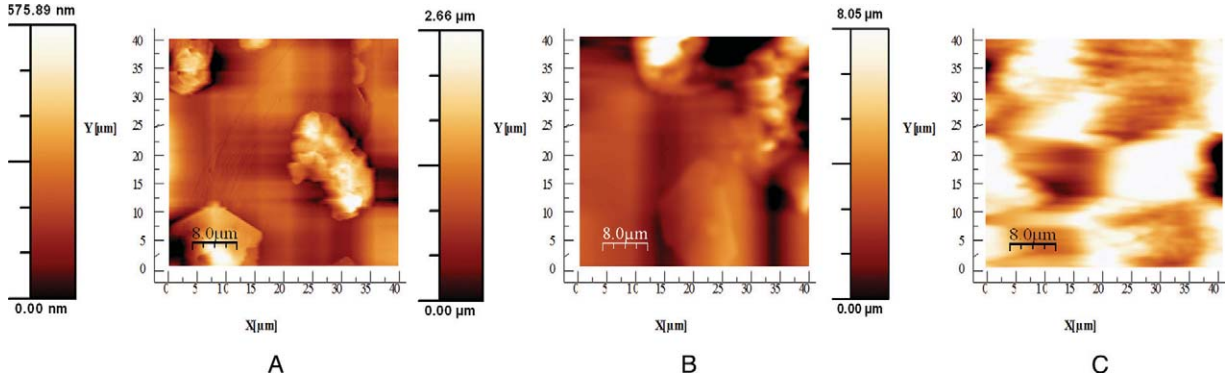

FIGURE 4. AFM images of IgG structures obtained by MAPLE deposition on fused silica substrates from IgG dissolved in water and saline buffer containing lipid at fluences of (A) 0.33 J/cm^2 (IL33), (B) 0.5 J/cm^2 (IL50), and (C) 0.67 J/cm^2 (IL67), respectively. [Color figure can be viewed in the online issue, which is available at wileyonlinelibrary.com.]

TABLE II. Roughness (RMS, Ra, and Rz) Values for All Samples

Sample	RMS (nm)	Ra (nm)	Rz (nm)
I33	160	124	681
I50	217	176	581
I67	139	101	522
IL33	109	83	147
IL50	271	177	697
IL67	1570	1314	4036

saturating concentration able to bind all deposited molecules of IgG only. The fluorescently labeled antibody was diluted 1:200, 1:50, and 1:25 and applied to both sample and control (fused silica substrate). Thirty-minutes or 1-h incubation time past in dark at room temperature, the samples were washed in PBS and scanned in 10 × 10 fields by spectrofluorimetry at 530-nm emission wavelength. To quantify, central squares (8 × 8) were averaged, and the intensity of fluorescence emission was recorded. Using 1:200 dilution of fluorescently labeled antibody, no difference was observed between substrate and sample. The 1:50 dilution has induced an increase in fluorescence emission of the samples while keeping the fused silica control at the same level of mean fluorescence intensity as in the previous dilution test. A total of 1:25 dilution of antibody has produced the same fluorescence intensity in either sample or control meaning the unspecific binding has occurred.

The results have been confirmed by fluorescence microscopy examination of the sample surfaces. The 1:50 dilution generated a myriad of fluorescent spots on the surface of IgG film but no signal on fused silica except autofluorescent defects on surface. In Figure 10(Ib,c), one can observe a heterogeneous distribution of small and larger dots situated in the center of sample I33 captured using either 10× or 40× objective versus fused silica control [Fig. 10(Ia)]. This observation explains the small increase in specific fluorescence because the emission is produced by discrete areas in the samples and not by a continuous film. There are two possible explanations for this phenomenon: either a very small amount of IgG molecules was transferred during the MAPLE procedure, or a percentage only of the deposited molecules were integer to be seen by the specific fluorescent secondary antibody. The most concentrated antibody solution (1:25) has caused unspecific binding of the fluorescently conjugated molecules to some sites in the fused silica control [Fig. 10(IIa)]. Moreover, an antibody capture by defects in the fused silica was observed (data not shown). An increase in the size of green spots was assessed on surface but not a multiplication of visible spots [Fig. 10(IIb,c)]. This offers an explanation of the increase in fluorescence measured by the fluorimeter. Hence, both fluorimetry and

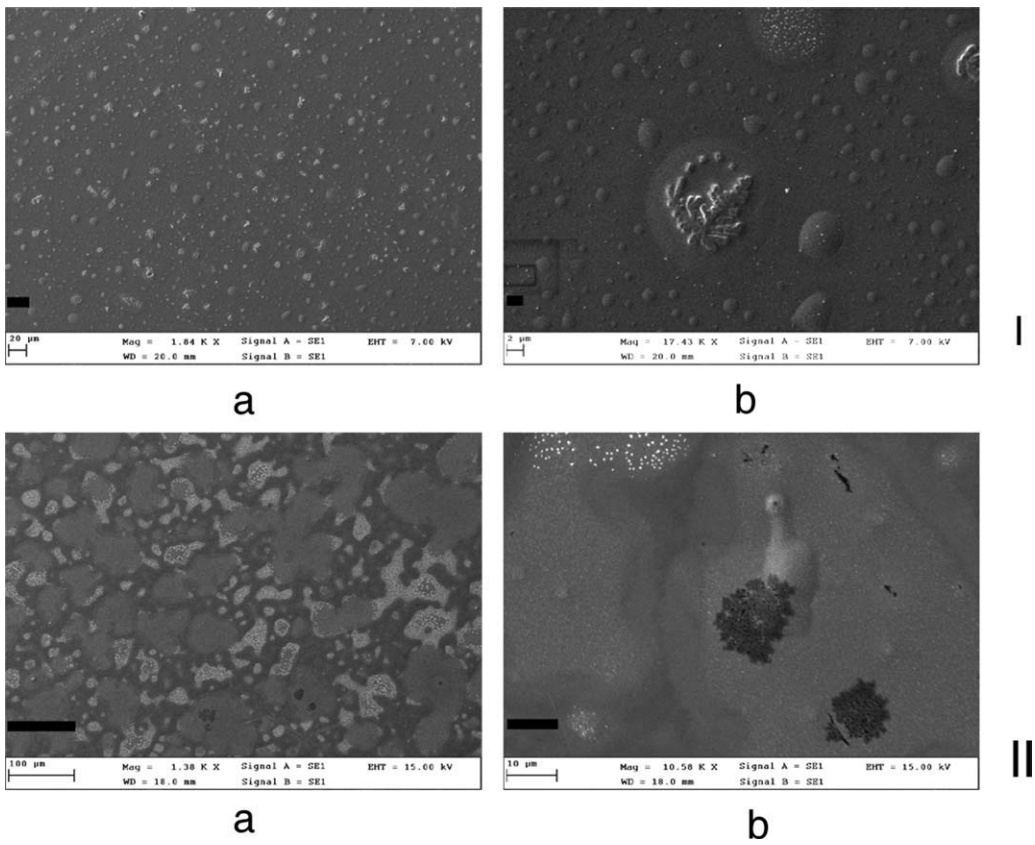

FIGURE 5. SEM images of IgG structures obtained by MAPLE from IgG dissolved in water and saline buffer without lipid (I33) (I) and containing lipid (IL33) (II) at fluence of 0.33 J/cm^2 at two different magnifications. Scale bars: Ia—20 μm, Ib—2 μm, IIa—100 μm, and IIb—10 μm.

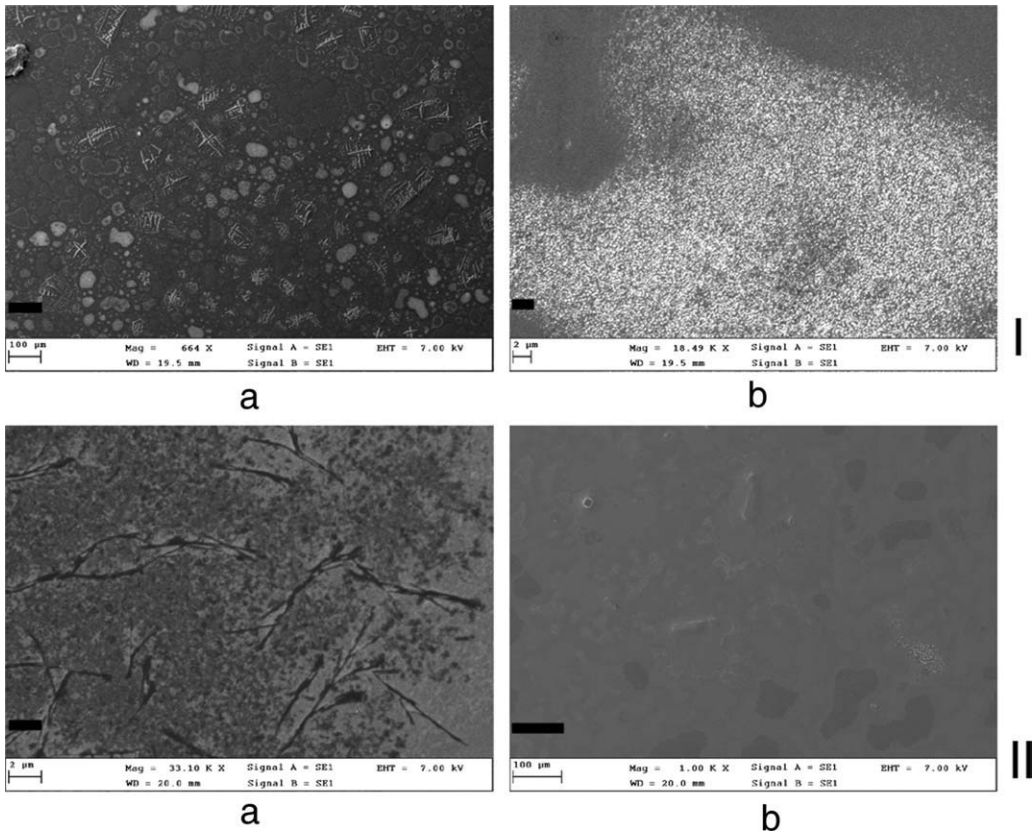

FIGURE 6. SEM images of IgG structures obtained by MAPLE from IgG dissolved in water and saline buffer without lipid (I50) (I) and containing lipid (IL50) (II) at fluence of 0.5 J/cm^2 at two different magnifications. Scale bars: Ia—100 μm, Ib—2 μm, IIa—2 μm, and IIb—100 μm.

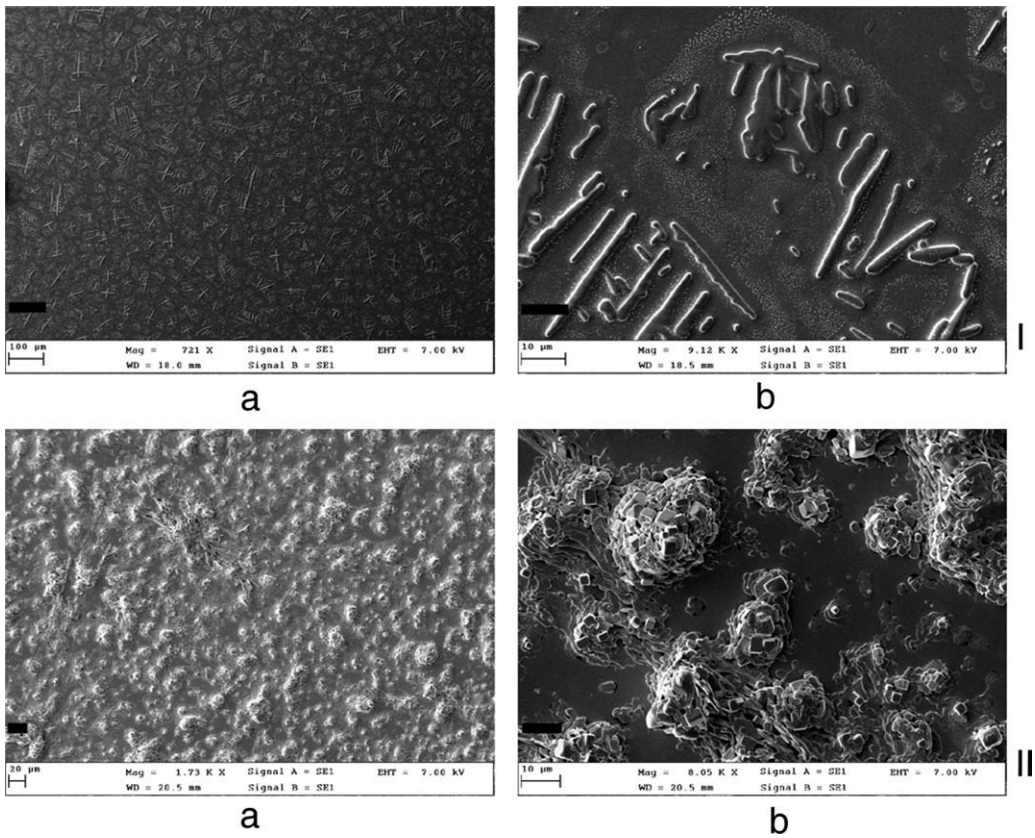

FIGURE 7. SEM images of IgG structures obtained by MAPLE from IgG dissolved in water and saline buffer without lipid (I67) (I) and containing lipid (IL67) (II) at fluence of 0.67 J/cm^2 at two different magnifications. Scale bars: Ia—100 μm, Ib—10 μm, IIa—20 μm, and IIb—10 μm.

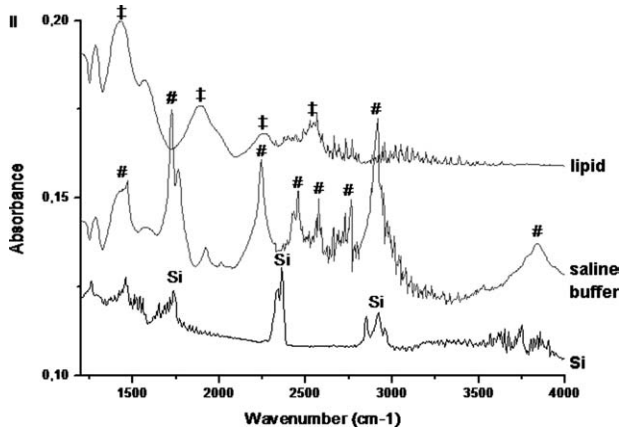

FIGURE 8. FTIR absorption spectra for Si, lipid (‡), and saline buffer (#) within the 1200–4000 cm^{-1} range.

microscopy data support the utilization of 1:50 antibody dilution to assay the qualitative difference between the three types of deposition parameters used.

We next incubated all samples with 1:50 dilution of Alexa Fluor 488 donkey anti-rabbit secondary antibody in blocking buffer. After 60 min, the samples were washed, scanned by fluorimetry, and examined under the fluorescent microscope.

Between the samples obtained from solutions without lipid, a slight tendency of I50 sample to emit a higher fluorescence was observed by spectrofluorimetry (Fig. 11). No uniform covering of the fused silica surface was assessed but rather a Schweitzer-like structure [Fig. 12(I50)] when compared with I67 samples where a rather continuous film [Fig. 12(I67)] was evidenced.

To increase the IgG molecule protection and immobilization to the substrates, we added lipid in the IgG solution used as MAPLE targets. To quantify the amount of IgG protein deposited on glass and fused silica substrates during transfer of lipid-added formulations, a BCA assay was performed using BSA dilutions as standard. The spectrophotometry data obtained for IL33, IL50, and IL67 samples have shown that the transfer efficiency increased with fluence. IL67 was found four times richer in antiserum proteins than IL50, independent of the substrate, whereas in the case of IL33 the protein presence could not be detected (Table III). In addition, a slight increase of protein amount could be noticed when using fused silica as a substrate.

One can observe from Figure 13 a uniform distribution with enhanced fluorescent areas of IgG-transferred material from solutions containing lipid, when compared with the samples deposited in the best regime from solutions without lipid.

DISCUSSION

The proteins can offer important advantages such as molecular recognition, self-assembly, or genetic manipulation.[25] The immobilization approaches regularly demand the use of specific surface functional groups having narrow capacity to be used for modification of most of materials. In consequence, there is a permanent need for flexible immobilization methods able to attach specific biomolecules to relevant material surfaces. Laser-assisted methods present some typical advantages over other techniques such as the accurate control of the layer thickness and/or expulsed material or the absence of contamination. They allow the uniform distribution of material over moderately large areas, and the extension to the synthesis of multistructures is rather easy. MAPLE process was particularly developed to provide a soft pulsed laser transfer of "delicate" (organic and/or biologic) materials. In our experiments, we used a pulsed UV (248 nm) excimer laser beam to irradiate a cryogenic target obtained after freezing by liquid nitrogen.

Laser transfer mechanism

As a consequence of laser transfer, IgG molecules remained immobilized on Si, glass, or fused silica substrates, as proved by repeated manipulation and immersion in liquid media. As for the mechanism, we assume that the laser beam energy was prevalently absorbed by the iced matrix (buffer solution) molecules and/or IgG biomolecules in the outer layer, heating the water in their surrounding area. At the target surface, the water boils and its vapors are transporting the IgG biomolecules on substrate surface where they remain immobilized.[26,27] During the transfer from target to substrate, the protection matrix and IgG molecules are sorting out. We note that according to Ref. 28,

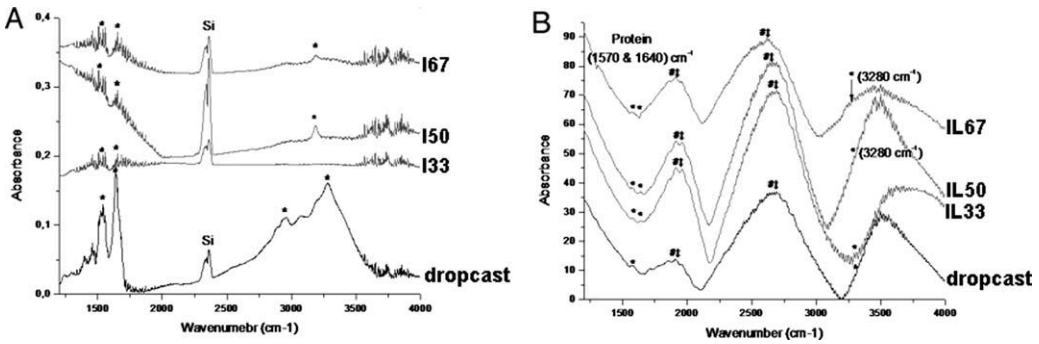

FIGURE 9. FTIR absorption spectra of (A) dropcast, I33, I50 and I67, and (B) dropcast, IL33, IL50, and IL67 within the 1200–4000 cm^{-1} range (*protein, #saline buffer, and ‡lipid).

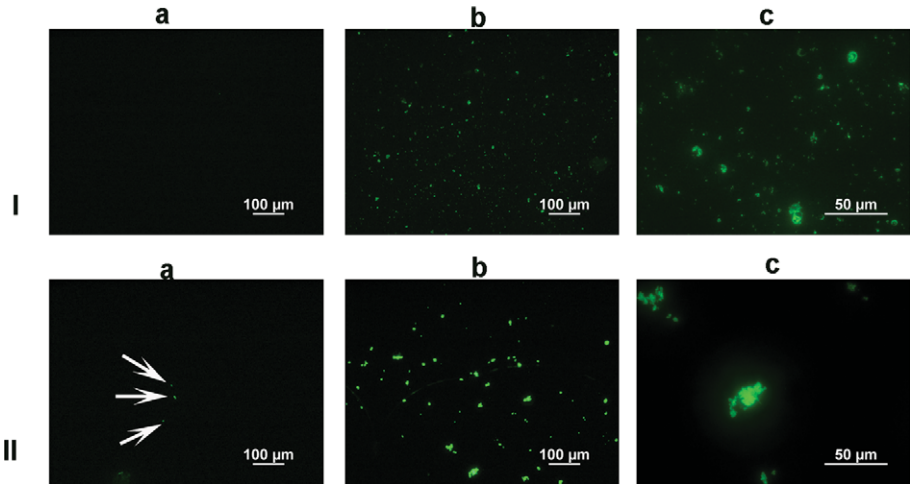

FIGURE 10. Fluorescence microscopy images of rabbit IgG samples after incubation with 1:50 (I) or 1:25 (II) dilution of Alexa Fluor-conjugated secondary antibody. [Color figure can be viewed in the online issue, which is available at wileyonlinelibrary.com.]

simulation studies showed that the active biomolecules are ejected in the ablation regime and incorporated into clusters produced during the development of the explosive disintegration of the overheated matrix. At an optimal separation distance, laser fluence, and pressure inside the reaction chamber, an important part of matrix molecules is purged out through the pumping system, while a fraction of them is driving the IgG molecules to the substrate (Fig. 14).

To improve the shielding protection of the protein structure and configuration and increase the adhesion of the transferred IgG to the substrate, 10 μL of lipid was introduced in 5 mL mere solution. A small fraction of lipid added in the started solution improved both the UV laser absorption by the matrix as demonstrated by the largest quantity of the transferred salts [Fig. 7(I) vs. 7(II)] as well as immobilization of the protein on the collecting substrate [Fig. 13(IL50) vs. 13(I50)].

Morphology compromise and estimated growth rate

Both protein adhesion to substrates and morphology strongly influence the reliability of a specific application. The morphology of the substrate also affects the biomolecule adhesion. This is why the morphological features stand for an important issue for biosensor application.[29]

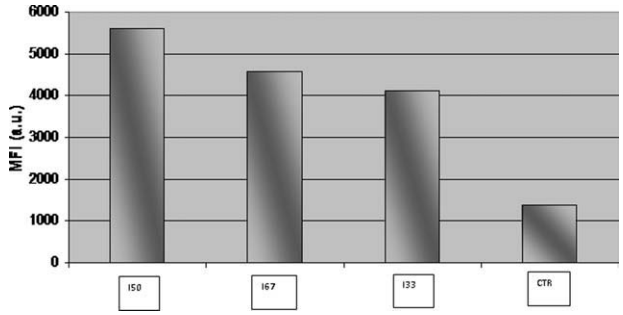

FIGURE 11. Fluorescence of rabbit IgG samples after incubation with 1:50 dilution of Alexa Fluor-conjugated secondary antibody (data are representative for one of three independent experiments using duplicates).

From our optical, atomic force and scanning microscopy investigations, it resulted that there is a "window" in laser fluence (~0.5 J/cm^2) for which the integer structure of the protein after expulsion and immobilization is preserved, and the morphology can be well controlled while an important quantity of material is transferred. The "window" is additionally significant as it not depends on lipid introduction in the mere buffered solution. The exit from this interval by reducing the laser fluence produces considerable loss of immobilized protein; while increasing it one can cause an important boost in surface roughness. The explanation for the significant increase of roughness from IL50 to IL67 (up to one order of magnitude) is the expulsion and deposition on the substrate of a larger amount of salt crystals in this latter case, when the highest incident laser fluence was applied for matrix evaporation (Fig. 7).

We estimated by AFM the average thickness of MAPLE-deposited structures. For the three laser fluences used, we obtained values of 200, 350, and 500 nm for lipid-free samples, and 180, 450, and 700 nm in the case of lipid-containing samples. This corresponds to a deposition rate of 0.02–0.05 nanometer per pulse in the first case and 0.018–0.07 nanometer per pulse in the second one, respectively. These results are in agreement with the data reported in Ref. 30 according to which the deposition rates in MAPLE are four to eight times lower than in PLD. Nevertheless, the direct PLD transfer of proteins like IgG is impossible; while

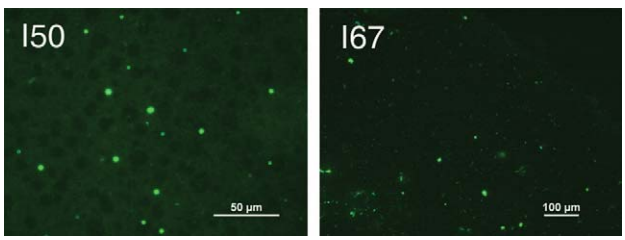

FIGURE 12. Fluorescence microscopy images of rabbit IgG samples after incubation with 1:50 dilution of Alexa Fluor-conjugated secondary antibody. [Color figure can be viewed in the online issue, which is available at wileyonlinelibrary.com.]

TABLE III. Quantification of IgG Protein Transferred by MAPLE Using Lipid-Added Formulations

IgG Structure	Glass Substrate	Fused Silica Substrate
IL33	Nondetectable	Nondetectable
IL50	1.03 μg	1.27 μg
IL67	4.10 μg	7.52 μg

the film morphology is quite convenient for MAPLE deposition application in biomedical purposes, as, for example, biosensors.

Composition preservation

From FTIR study of IgG dropcast spectrum in Figure 9(A), we identified the main protein absorption lines at 1539, 1640, 2962, and 3280 cm^{-1}, respectively. According to literature, the peak around 1640 cm^{-1} corresponded to amide I band of protein secondary structure,[31–33] whereas the line at 1539 cm^{-1} could be assigned to amide II/II′ bands.[31,32] Also, the peak at 2962 cm^{-1} belonged to ν(CH3) and ν(CH2) vibrations,[34] and the line at 3280 cm^{-1} was probably due to amide A and H_2O absorption superposed to OH stretch.[34]

The sensor transduction principle

The conformational stability of the transferred IgG molecules was demonstrated by optical labeling methods such as fluorescence microscopy and spectrofluorimetry. A 1:50 dilution of Alexa Fluor 488 donkey anti-rabbit secondary antibody in blocking buffer was chosen as it produced a multitude of fluorescent spots on the surface of IgG film but no signal on fused silica control.

Even though among the samples prepared from lipid-free solutions, a tendency of I50 to emit a higher fluorescence was observed, no uniform covering of the fused silica surface was evidenced. A rather Schweitzer-like structure was noticed perhaps because of immobilization deficiencies of the film when immersed in the antibody solution. Introducing a lipid in the initial solution, the structure obtained in case of I50 was replaced with a uniform continuous film (IL50), which means the immobilization of IgG molecules was significantly improved by addition of lipid (Fig. 13). The regions of increased intensity could be owed to protein aggregates with improved adhesion to the substrate.

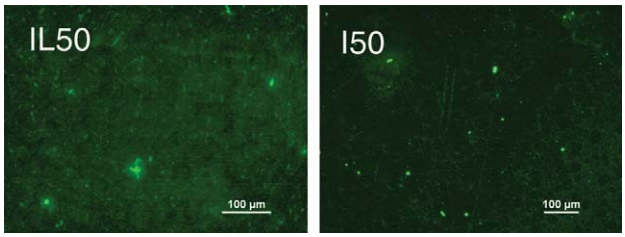

FIGURE 13. Fluorescence microscopy images of rabbit IL50 versus I50 samples after incubation with 1:50 dilution of Alexa Fluor-conjugated secondary antibody. [Color figure can be viewed in the online issue, which is available at wileyonlinelibrary.com.]

On the basis of this study, we advance the suggestion of using MAPLE-immobilized IgG films as immunosensors for the detection of specific antigens in research or clinical investigations. To this prospective, the observed possibility to control the sensor surface morphology by the content of salts and lipid in MAPLE solutions confers a large avenue for finding the best compromise between the IgG content and surface condition over sensing capabilities. This can stand for an essential step in developing personalized and miniaturized biosensors. Although laser-induced forward transfer already proved a versatile tool in view of obtaining

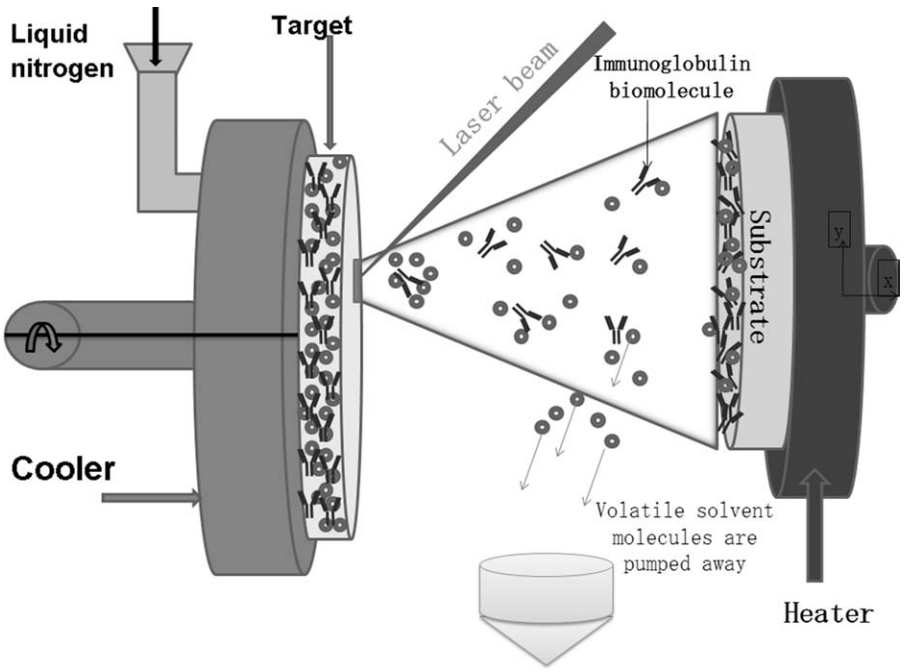

FIGURE 14. Scheme of MAPLE transfer of protein molecules.

defined patterns,[35] one can see the potential of using specific masks or photomasks[36] in MAPLE experiments to synthesize well-controlled microsized samples for microarray chip applications. Microchip-based immunoassay devices would facilitate a supplementary degree of complexity achieved with difficulty by the current flow-through membrane-based immunoassay devices.

CONCLUSION

We transferred and immobilized by MAPLE IgG thin films onto glass, fused silica, or silicon substrates. The introduction of lipid in the solution proved beneficial for the process efficiency. The physical–chemical analyses (optical microscopy, AFM, SEM, and FTIR) evidenced an optimal protection regime of protein transfer for the intermediate incident laser fluence of 0.5 J/cm^2. BCA assay demonstrated an obvious increase of protein amount in deposited films with the incident laser fluence increasing from 0.33 to 0.67 J/cm^2. There is, however, a "window" in laser fluence ($\sim$0.5 J/cm^2) for which the integer structure of the protein was preserved and morphology can be well controlled. A larger amount of protein was detected in structures deposited on fused silica. The tunable approach of all parameters could be essential in developing a performant immunosensor for versatile applications.

REFERENCES

1. Decher G, Hong JD, Schmitt J. Buildup of ultrathin multilayer films by a self-assembly process. III. Consecutively alternating adsorption of anionic and cationic polyelectrolytes on charged surfaces. Thin Solid Films 1992;210:831–835.
2. Yang W, Trau D, Renneberg R, Yu NT, Caruso F. Layer-by-layer construction of novel biofunctional fluorescent microparticles for immunoassay applications. J Colloid Interface Sci 2001;234:356–362.
3. Blodgett KB. Monomolecular films of fatty acids on glass. J Am Chem Soc 1934;56:495.
4. Wu Z, Ding L, Chen H, Yuan L, Huang H, Song W. Immobilization of proteins on metal ion chelated polymer surfaces. Colloids Surf B 2009;69:71–76.
5. Vareiro MMLM, Liu J, Knoll W, Zak K, Williams D, Jenkins ATA. Surface plasmon fluorescence measurements of human chorionic gonadotrophin: Role of antibody orientation in obtaining enhanced sensitivity and limit of detection. Anal Chem 2008;77:2426–2431.
6. Briand E, Salmain M, Compere C, Pradier CM. Immobilization of Protein A on SAMs for the elaboration of immunosensors. Colloids Surf B 2006;53:215–224.
7. Ha TH, Jung SO, Lee JM, Lee KY, Lee Y, Park JS, Chung BH. Oriented immobilization of antibodies with GST-fused multiple Fc-specific B-domains on a gold surface. Anal Chem 2007;79:546–556.
8. Betancor L, Lopez-Gallego F, Hidalgo A, Alonso-Morales N, Dellamora-Ortiz Cesar Mateo G, Fernandez-Lafuente R, Guisan JM. Different mechanisms of protein immobilization on glutaraldehyde activated supports: Effect of support activation and immobilization conditions. Enzyme Microb Technol 2006;39:877–882.
9. Raj J, Herzog G, Manning M, Volcke C, MacCraith BD, Ballantyne S, Thompson M, Arrigan DWM. Surface immobilisation of antibody on cyclic olefin copolymer for sandwich immunoassay. Biosens Bioelectron 2009;24:2654–2658.
10. Weiping Q, Bin X, Lei W, Chunxiao W, Danfeng Y, Fang Y, Chunwei Y, Yu W. Controlled site-directed assembly of antibodies by their oligosaccharide moieties onto APTES derivatized surfaces. J Colloid Interface Sci 1999;214:16–19.
11. Lee LM, Heimark RL, Baygents JC, Zohar Y. Self-aligned immobilization of proteins utilizing PEG patterns. Nanotechnology 2006;17: S29–S33.
12. Dreesen L, Humbert Ch, Sartenaer Y, Caudano Y, Volcke C, Mani AA, Peremans A, Thiry PA, Hanique S, Frere JM. Electronic and molecular properties of an adsorbed protein monolayer probed by two-color sum-frequency generation spectroscopy. Langmuir 2004;20:7201–7207.
13. Sethuraman A, Han M, Kane RS, Belfort G. Effect of surface wettability on the adhesion of proteins. Langmuir 2004;20: 7779–7788.
14. Xu H, Zhao X, Grant C, Lu JR, Williams DE, Penfold J. Orientation of a monoclonal antibody adsorbed at the solid/solution interface: A combined study using atomic force microscopy and neutron reflectivity. Langmuir 2006;22:6313–6320.
15. Piqué A, McGill RA, Chrisey DB, Leonhardt D, Mslna TE, Spargo BJ, Callahan JH, Vachet RW, Chung R, Bucaro MA. Growth of organic thin films by the matrix assisted pulsed laser evaporation (MAPLE) technique. Thin Solid Films 1999;355/356:536–541.
16. Pique A. Deposition of polymers and biomaterials using the matrix assisted pulsed laser evaporation (MAPLE) process. In: Eason R, editor. Pulsed Laser Deposition of Thin Film. New Jersey: Wiley; 2006. p 63–84.
17. Mihailescu IN, Ristoscu C, Bigi A, Mayer I. Advanced biomimetic implants based on nanostructured coatings synthesized by pulsed laser technologies. In: Miotello A, Ossi PM, editors. Laser-Surface Interactions for New Materials Production Tailoring Structure and Properties. Heidelberg, Dordrecht, London, New York: Springer. 2010. p 235–260.
18. Cristescu R, Stamatin I, Mihaiescu DE, Ghica C, Albulescu M, Mihailescu IN, Chrisey DB. Pulsed laser deposition of biocompatible polymers: A comparative study in case of pullulan. Thin Solid Films 2004;453/454:262.
19. Cristescu R, Doraiswamy A, Socol G, Grigorescu S, Axente E, Sima F, Narayan RJ, Mihaiescu D, Moldovan A, Stamatin I, Mihailescu IN, Chisholm BJ, Chrisey DB. Polycaprolactone biopolymer thin films obtained by matrix assisted pulsed laser evaporation. Appl Surf Sci 2007;25:6476–6479.
20. Gyorgy E, Sima F, Mihailescu IN, Smausz T, Megyeri G, Kekesi R, Hopp B, Zdrentu L, Petrescu SM. Immobilization of urease by laser techniques: Synthesis and application to urea biosensors. J Biomed Mater Res A 2009;89:186–191.
21. Gyorgy E, Sima F, Mihailescu IN, Smauz T, Hopp B, Predoi D, Sima LE, Petrescu SM. Biomolecular urease thin films grown by laser techniques for blood diagnostic applications. Mater Sci Eng C 2010;30:537–541.
22. Purice A, Schou J, Kingshott P, Dinescu M. Production of active lysozyme films by matrix assisted pulsed laser evaporation at 355 nm. Chem Phys Lett 2007;435:350–353.
23. Duschl C, Hall EAH. Adsorption and complex formation of immunoglobulins on silicon wafers, studied by interference-enhanced reflectometry. J Colloid Interface Sci 1991;144:368–380.
24. de Bartolo L, Morelli S, Bader A, Driolia E. Evaluation of cell behaviour related to physico-chemical properties of polymeric membranes to be used in bioartificial organs. Biomaterials 2002; 23:2485–2497.
25. Tamerler C, Sarikaya M. Molecular biomimetics: Utilizing nature's molecular ways in practical engineering. Acta Biomater 2007;3: 289–299.
26. Gyorgy E, del Pino A, Sauthier G, Figueras A. Biomolecular papain thin films grown by matrix assisted and conventional pulsed laser deposition: A comparative study. J Appl Phys 2009;106:114702–1–114702–6.
27. Smausz T, Megyeri G, Kekesi R, Vass C, Gyorgy E, Sima F, Mihailescu IN, Hopp B. Comparative study on pulsed laser deposition and matrix assisted pulsed laser evaporation of urease thin films. Thin Solid Films 2009;517:4299–4302.
28. Leveugle E, Zhigilei LV. Molecular dynamics simulation study of the ejection and transport of polymer molecules in matrix-assisted pulsed laser evaporation. J Appl Phys 2007;102:074914–1–074914–19.
29. Bhushan B, Tokachichu DR, Keener MT, Lee SC. Morphology and adhesion of biomolecules on silicon based surfaces. Acta Biomater 2005;1:327–341.
30. Jelinek M, Kocourek T, Remsa J, Cristescu R, Mihailescu IN, Chrisey DB. MAPLE applications in studying organic thin films. Laser Phys 2007;17:66–70.

31. Goormaghtigh E, Cabiaux V, Ruysschaert JM. Determination of soluble and membrane protein structure by Fourier transform infrared spectroscopy. III. Secondary structures. In Hilderson HJ, Ralston GB, editors. Subcellular Biochemistry. New York: Plenum; 1994. p 405–450.
32. Bandekar J. Amide modes and protein conformation. Biochim Biophys Acta 1992;1120:123–143.
33. Giacomelli CE, Bremer MGEG, Norde W. ATR-FTIR study of IgG adsorbed on different silica surfaces. J Colloid Interface Sci 1999; 220:13–23.
34. Jung C. Insight into protein structure and protein-ligand recognition by Fourier transform infrared spectroscopy. J Mol Recognit 2000;13:325–351.
35. Kononenko TV, Nagovitsyn IA, Chudinova GK, Mihailescu IN. Application of clean laser transfer for porphyrin micropatterning. Appl Surf Sci 2010;256:2803–2808.
36. Ito Y, Hasuda H, Sakuragi M, Tsuzuki S. Surface modification of plastic, glass and titanium by photoimmobilization of polyethylene glycol for antibiofouling. Acta Biomater 2007;3:1024–1032.